Synthesis of block copolymers using poly(methyl methacrylate) with unsaturated chain end through kinetic studies

Chang, Jun Jie; Niino, Hiroshi; Chatani, Shunsuke; Goto, Atsushi

2019

Chang, J. J., Niino, H., Chatani, S., & Goto, A. (2019). Synthesis of block copolymers using poly(methyl methacrylate) with unsaturated chain end through kinetic studies. Polymer Chemistry, 10(41), 5617-5625. doi:10.1039/c9py01367a

https://hdl.handle.net/10356/137721

https://doi.org/10.1039/c9py01367a

ARTICLE

Synthesis of Block Copolymers Using Poly(methyl methacrylate) with Unsaturated Chain End through Kinetic Studies

Received 00th January 20xx,
Accepted 00th January 20xx

DOI: 10.1039/x0xx00000x

Jun Jie Chang,[a] Hiroshi Niino,[b] Shunsuke Chatani,[b] and Atsushi Goto*[a]

A poly(methyl methacrylate) (PMMA) with an unsaturated chain end (PMMA–Y) was used as a macroinitiator in the polymerizations of several monomers to generate block copolymers *via* addition-fragmentation chain transfer (AFCT). PMMA–Y also worked as a macromonomer to generate branched polymers *via* propagation. A kinetic study revealed that the occurrence of AFCT and propagation significantly depends on temperature in the styrene polymerization; namely, while progapation was predominant below 60 °C as previously reported, AFCT was predominant at elevated temperatures such as 120 °C as newly revealed in the present work. This new kinetic finding opened up an efficient synthesis of block copolymers of PMMA with polystyrene at an elevated temperature. AFCT was also predominant over propagation in the polymerizations of acrylonitrile and acrylates. Thus, block copolymers of PMMA with polyacrylonitrile and functional polyacrylates were successfully obtained. The polymerization was controlled using iodine transfer polymerization (ITP) for styrene and reversible complexation mediated polymerization (RCMP) for the other monomers. PMMA–Y with different molecular weights were also tested. This approach to obtain block copolymers is practically attractive for the ease of operation.

Introduction

Living radical polymerization (LRP), also termed reversible-deactivation radical polymerization, is a versatile method to synthesize polymers with predictable molecular weights and narrow molecular weight distributions and also importantly synthesize block copolymers.[1–9] Our research group developed an organocatalyzed LRP using alkyl iodides (R–I) as initiators and organic molecules as catalysts (Scheme 1).[10–16] In this LRP, polymer-iodide dormant species (polymer–I) coordinates a catalyst *via* halogen bonding to form a complex (polymer–I···catalyst). The complex reversibly generates a propagating radical (Polymer$^{\bullet}$). We termed this polymerization as reversible complexation mediated polymerization (RCMP). The catalysts include organic salts such as tetrabutylammonium iodide ($Bu_4N^+I^-$ (BNI)).[11] This polymerization is attractive for no use of special capping agents or expensive catalysts and for amenability to a wide range of monomers and polymer structures.

Polymer–I can function as a macroinitiator to synthesize block copolymers. However, owing to a weak carbon-iodide bond, polymer–I is generally not very stable upon long-term storage.[6,17] We recently reported the use of a poly(methyl methacrylate) (PMMA) containing an unsaturated chain end (PMMA–Y) as a macroinitiator in RCMP of butyl acrylate (BA), where Y is $CH_2CH(=CH_2)COOCH_3$ (Scheme 2).[18] PMMA–Y is typically prepared *via* cobalt-mediated catalytic chain-transfer polymerization.[19–23] PMMA–Y was converted to PMMA$^{\bullet}$ *via* an addition fragmentation chain transfer (AFCT)[23–32] of a poly(butyl acrylate) radical (PBA$^{\bullet}$) to PMMA–Y (Scheme 2a). The generated PMMA$^{\bullet}$ subsequently added BA monomers to yield a PMMA–PBA block copolymer in one pot. Because PMMA–Y is stable under long-term storage, its use as a macroinitiator is a convenient and practical method to obtain block copolymers.

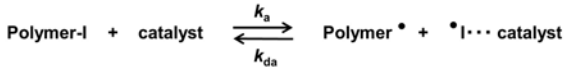

Scheme 1 Reversible activation in RCMP.

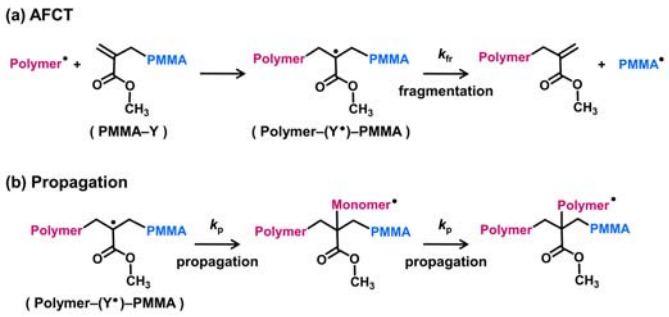

Scheme 2 (a) AFCT (addition-fragmentation chain transfer) *via* the fragmentation of the intermediate radical and (b) propagation of the intermediate radical.

[a] *Division of Chemistry and Biological Chemistry, School of Physical and Mathematical Sciences, Nanyang Technological University, 21 Nanyang Link, 637371 Singapore. E-mail: agoto@ntu.edu.sg*
[b] *Otake R&D Center, Mitsubishi Chemical Corporation, 20-1 Miyuki-cho, Otake, Hiroshima 739-0693, Japan.*

Electronic Supplementary Information (ESI) available: Experimental section and MALDI-TOF-MS data. See DOI: 10.1039/x0xx00000x

PMMA–Y can also act as a macromonomer. A propagating radical (Polymer$^{\bullet}$) adds to the C=C double bond of PMMA–Y to generate the intermediate radical Polymer–(Y$^{\bullet}$)–PMMA (Scheme 2). When PMMA$^{\bullet}$ is fragmented, the process is AFCT (Scheme 2a). When the intermediate radical adds to a monomer, the process is propagation, generating a branched polymer (Scheme 2b). In this paper, we define the fragmentation rate constant as k_{fr} (Scheme 2a), the propagation rate constant as k_p (Scheme 2b), and the fraction of the intermediate radical to undergo the fragmentation as F_{fr} = $k_{fr}/(k_{fr}+k_p)$. In the case of polyacrylate radicals for Polymer$^{\bullet}$, AFCT is predominant (F_{fr} > 90%) over propagation.[26] In the case of polystyrene radical (PSt$^{\bullet}$), it was reported that AFCT is less significant (F_{fr} > 40%) than propagation at 60 °C.[26]

In this work, we experimentally determined F_{fr} for several different Polymer$^{\bullet}$, i.e., PSt$^{\bullet}$, poly(acryronitrile) radical (PAN$^{\bullet}$), and functional hydrophobic and amphiphilic polyacrylate radicals. A significant finding was that AFCT became predominant (F_{fr} ~ 100%) over propagation at an elevated temperature (120 °C) for PSt$^{\bullet}$, which is in sharp contrast to the F_{fr} value (> 40%) at 60 °C, showing a markedly large temperature dependence of F_{fr}. This kinetic finding opened up the use of PMMA–Y as a macroinitiator to produce PMMA–PSt block copolymers by simply elevating temperature, which was unable to be achieved at mild temperatures such as 60 °C. AFCT was also predominant (F_{fr} > 90%) for PAN$^{\bullet}$ and the studied functional polyacrylate radicals, enabling the synthesis of block copolymers. This work successfully expanded the monomer scope for the synthesis of block copolymers from PMMA–Y. We also studied PMMA–Y with different molecular weights. The high stability of PMMA–Y upon storage and the encompassed monomer scope including important monomer families (acrylates, styrene (St), and acrylonitrile (AN)) with functional groups are attractive features in this approach.

Results and Discussion

Temperature Dependence of F_{fr} for PSt$^{\bullet}$ and PMMA–Y

We used a PMMA–Y with M_n = 3900 and dispersity $Đ$ (= M_w/M_n) = 1.67, where M_n and M_w are the number-average and weight-average molecular weights, respectively. We carried out bulk polymerizations of St (200 equiv) with PMMA–Y (1 equiv), a conventional radical initiator (peroxide or azo initiator) (0.3–10 equiv), and 2-iodo-2-methylpropionitrile (CP–I) (1 equiv) (Fig. 1) at different temperatures (40–120 °C) (Table S1 in the ESI). CP–I was added as an alkyl iodide dormant species of LRP (iodide transfer polymerization (ITP)[6] in the styrene system) to control the molecular weight.

The conventional radical initiator generates radicals, which react with St to form PSt$^{\bullet}$. PSt$^{\bullet}$ undergoes addition to the C=C double bond of PMMA–Y to form the intermediate radical PSt–(Y$^{\bullet}$)–PMMA, which can undergo fragmentation or propagation (Scheme 2). After the reaction, the polymer was purified with a preparative gel permeation chromatography (GPC) to remove small molecules such as residual monomer and radical initiator. Fig. 2 shows the ^{1}H NMR spectra ($CDCl_3$) of the polymers obtained at time zero (Fig. 2a) and 10 min (Fig. 2b, monomer conversion = 10%) at 120 °C. The resonance peaks of CH_2=C of PMMA–Y were observed at 5.45–5.53 and 6.18–6.23 ppm (Fig. 2a). Through the fragmentation, the Y group is transferred from PMMA–Y to PSt$^{\bullet}$, generating PSt–Y (Scheme 2a). At 10 min, two new resonances appeared at 5.03–5.15 and 5.88–5.98 ppm and corresponded to the CH_2=C of PSt–Y (Fig. 2b).[33] Thus, the AFCT of PMMA–Y to generate PSt–Y was clearly observed. The formation of PSt–Y was also confirmed by matrix assisted laser desorption/ionization time-of-flight mass spectrometry (MALDI-TOF-MS) (Fig. S1 in the ESI). In the NMR spectra (Fig. 2), the decay in PMMA–Y corresponds to the sum of k_{fr} and k_p, and the generation of PSt–Y corresponds to k_{fr}. We followed the change in the CH_2=C peak areas of PMMA–Y and PSt–Y using the OCH_3 peak area of PMMA as an internal standard (which was unchanged during the reaction) and obtained the F_{fr} value (= $k_{fr}/(k_{fr}+k_p)$).

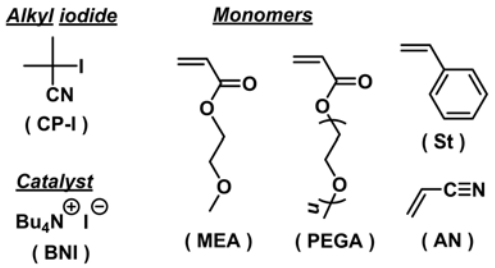

Fig. 1 Structures of alkyl iodide, catalyst, and monomers used in this work.

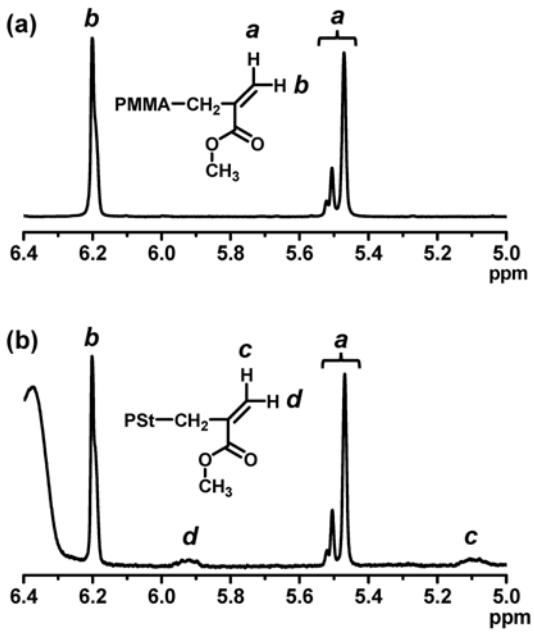

Fig. 2 ^{1}H NMR spectra ($CDCl_3$) in the range of 5.0–6.4 ppm at t = (a) 0 and (b) 10 min for the St/PMMA–Y/CP–I/PBZ system (120 °C) (Table S1 (entry 6) in the ESI); $[St]_0/[PMMA–Y]_0/[CP–I]_0/[PBZ]_0$ = 8000/40/40/40 (mM). PBZ is *tert*-butyl peroxybenzoate.

Fig. 3 shows the F_{fr} values obtained at different temperatures. In this kinetic study, we intentionally focused on low monomer conversion regions (i.e., below 15% monomer conversion), because the generated PSt–Y can be consumed as a macromonomer during the polymerization, which causes an underestimation of the F_{fr} value. For the same reason, we also extrapolate the plots (Fig. 3). The F_{fr} value extrapolated at the zero monomer conversion should be the most reasonable and is summarized in Table 1 (entry 1). The F_{fr} value determined at 60 °C was 38%, which is consistent with the literature value (40%) at 60 °C (Table 1 (entry R2)).

A significant finding was that the F_{fr} value markedly increased with an increase in temperature and that the fragmentation is predominant over propagation (F_{fr} ~ 100%) at 120 °C. This finding opens up the use of PMMA–Y to produce PMMA–PSt block copolymers by simply elevating temperature, as demonstrated below, which was unable to achieve at 60 °C. Conversely, the fragmentation occurred only 13% at 40 °C. Therefore, PMMA–PSt block copolymers are obtainable at 120 °C, while branched copolymers are obtainable as the major products at 40 °C, which will be discussed below.

Because the fragmentation of the PSt–(Y$^{\bullet}$)–PMMA intermediate radical is a bond breaking process, a greater energy would be required compared with the propagation (radical addition), which is a bond forming process. At the same time, fragmentation is entropically favored at higher temperatures ($\Delta S > 0$) compared to propagation ($\Delta S < 0$). This would rationalize the promoted fragmentation with an increase in temperature. Fig. 4 shows the Arrhenius plot of the ratio of k_{fr}/k_p (not $F_{fr} = k_{fr}/(k_{fr}+k_p)$). The k_{fr}/k_p value at 120 °C is not included, because F_{fr} was nearly 100% and hence k_{fr}/k_p becomes mathematically infinity. The plot gives equation (1).

$$k_{fr}/k_p = 3.8 \times 10^5 \exp(-37.4 \text{ kJ mol}^{-1}/RT) \quad (1)$$

The activation energy of 37.4 kJ mol^{-1} is the energy difference between the two processes ($E_{fr} - E_p$).

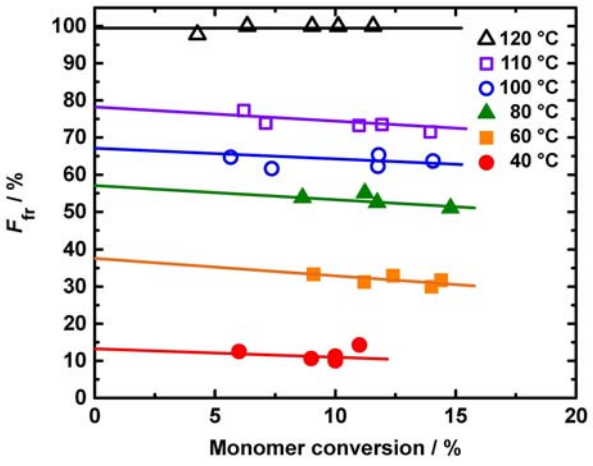

Fig. 3 Plot of F_{fr} vs monomer conversion for the St/PMMA–Y systems at 40–120 °C (Table S1 in the ESI). The symbols are indicated in the figure.

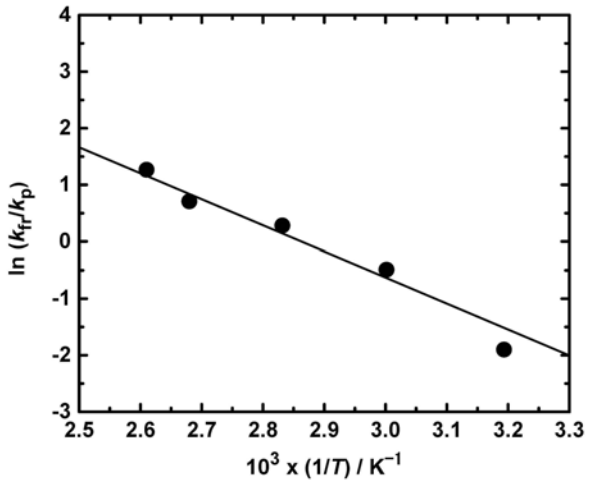

Fig. 4 Arrhenius Plot of k_{fr}/k_p for the St/PMMA–Y system.

Table 1 F_{fr} values for PMMA–Y with Polymer$^{\bullet}$.

Entry	R–Y	Polymer$^{\bullet}$	T (°C)	F_{fr} (%)	Ref.
R1	PMMA–Y	PMA$^{\bullet}$	60	>90	26
R2		PSt$^{\bullet}$	60	>40	26
1	PMMA–Y	PSt$^{\bullet}$	40	13	This work
			60	38	This work
			80	57	This work
			100	67	This work
			110	78	This work
			120	~100	This work
2	PMMA–Y	PAN$^{\bullet}$	75	97	This work
3	PMMA–Y	PMEA$^{\bullet}$	110	~100	This work
4	PMMA–Y	PPEGA$^{\bullet}$	110	83	This work

Table 2. Polymerizations using PMMA–Y (M_n = 3900 and $Đ$ = 1.67).

Entry	monomer	In[a]	[Monomer]$_0$/[PMMA–Y]$_0$/ [CP–I]$_0$/[In]$_0$/[BNI]$_0$ (mM)	T (°C)	t (h)	Conv (%)	M_n[b] ($M_{n,theo}$[c])	$Đ$[b]
1	St	PBZ	8000/40/40/60/0	120	15 min	24	4600 (8900)	2.00
					30 min	46	8500 (13000)	1.77
					1	56	14000 (16000)	1.63
					3	96	17000 (24000)	1.60
2	St	V65	8000/40/40/400/0	40	16	90	15000 (23000)	1.51
3	AN	AIBN	8000/40/40/4/160[d]	75	1	46	5900 (8800)	1.74
					3	67	7900 (11000)	1.90
					5	83	14000 (13000)	2.04
					7	86	15000 (13000)	1.82
4	MEA	none	8000/40/40/0/320	110	2	17	4400 (8300)	1.48
					4	27	5600 (11000)	1.47
					8	45	7900 (16000)	1.61
					16	69	12000 (22000)	1.86
					24	72	15000 (23000)	1.96
5	PEGA	none	8000/80/80/0/640	110	2	12	7700 (9700)	1.25
					4	17	8700 (12000)	1.26
					8	23	9300 (15000)	1.28
					16	34	12000 (20000)	1.41
					24	41	13000 (24000)	1.53

[a]Conventional radical initiator. PBZ = *tert*-butyl peroxybenzoate (PBZ), V65 = 2,2'-azobis(2,4-dimethylvaleronitrile), and AIBN = 2,2-azobis(2-methylpropionitrile) (AIBN). [b]PMMA-calibrated GPC values. The eluent was tetrahydrofuran (THF) for entries 1, 2 and 4 and dimethylformamide (DMF) for entries 3 and 5. [c]Theoretical M_n calculated with [monomer]$_0$, [PMMA–Y]$_0$, and monomer conversion. [d]Diluted in 50 wt% ethylene carbonate (EC).

Block polymerization of St from PMMA–Y.

The mentioned kinetic finding inspired us to study the block polymerization of St using PMMA–Y at an elevated temperature of 120 °C. We heated a mixture of St (200 equiv), PMMA–Y (M_n = 3900 and $Đ$ = 1.67) (1 equiv), *tert*-butyl peroxybenzoate (PBZ) (conventional radical initiator) (1.5 equiv), and CP–I (1 equiv) at 120°C (Table 2 (entry 1) and Fig. 5a). This is ITP including CP–I as an alkyl iodide dormant species but without catalysts. As Fig. 5a shows, the GPC curve shifted from the low molecular weight to high molecular weight side with an increase in the polymerization time. After 3 h, the monomer conversion reached 96%, M_n was 17000, and $Đ$ was 1.60 (Table 2 (entry 1) and Figs. 5a and 5b). In order to confirm the generation of the PMMA–PSt block copolymer, we fractionated a higher-molecular-weight species (molecular weight >5000) (green shaded region in Fig. 5b) from the original PMMA–Y (M_n = 3900) using a preparative GPC and analyzed the higher-molecular-weight species with ^{1}H NMR (Fig. 5c). Both PMMA (3.50–3.70 ppm for OCH_3) and PSt (6.25–7.50 ppm for C$_6H_5$) segments were observed, confirming the successful formation of the PMMA–PSt block copolymer.

Fig. 6 shows the monomer conversion and the amounts of PMMA–Y and PSt–Y at different times. PMMA–Y gradually decayed and was nearly completely consumed after 1 h (monomer conversion = 56%) (Fig. 6b), suggesting that nearly all of the PMMA–Y chains became PMMA–PSt block copolymers. PSt–Y was accumulated at the initial stages of polymerization and started to decay after 30 min (monomer conversion = 46%) (Fig. 6c), meaning that the generated PSt–Y was consumed as a macromonomer in the St polymerization. Therefore, the PSt segment in the block copolymer could contain PSt branches originated from PSt–Y. Because one PMMA–Y generates one PSt–Y (macromonomer), the block polymer can contain approximately one PSt branch in a PSt segment on average.

Scheme 3 illustrates the polymerization behaviour. PMMA–Y, CP–I, and St generate PMMA–PSt–I and PSt–Y through the consumption of PMMA–Y *via* AFCT (step 1). The PSt segment of the block copolymer subsequently grows in a controlled manner *via* LRP (step 2). The PSt block segment can add to PSt–Y and contain a PSt branch.

A possible deviation in the actual polymerization is the concurrent occurrence of steps 1 and 2. Because PMMA–Y was gradually consumed, step 1 gradually shifted to step 2. Hence, the AFCT of PMMA–PSt$^\bullet$ to PMMA–Y can also occur to generate another macromonomer, i.e., PMMA–PSt–Y. The gradual consumption of PMMA–Y also means non-uniform initiation from the PMMA chain. The distribution of the number of PSt branches per block copolymer chain is also random, while the average is one (as mentioned). These unavoidable deviations explain the observed larger $Đ$ values ($Đ$ > 1.60) (Table 2 (entry 1)) than those ($Đ$ < 1.5) in usual living systems.

The addition of catalysts (converting ITP to RCMP) did not significantly lower the $Đ$ value in this styrene system. Because of the mentioned unavoidable deviations, it seems that the $Đ$ value of 1.60 attained by this ITP system is already close to the lowest achievable value and hence was not able to be lowered even though the addition of catalyst could give a larger number of activation-deactivation cycles. In contrast, in the AN and acrylate systems described below, because the frequency

of the iodide transfer (ITP) is not high enough, the addition of catalysts (RCMP) was effective to lower the *Đ* value.

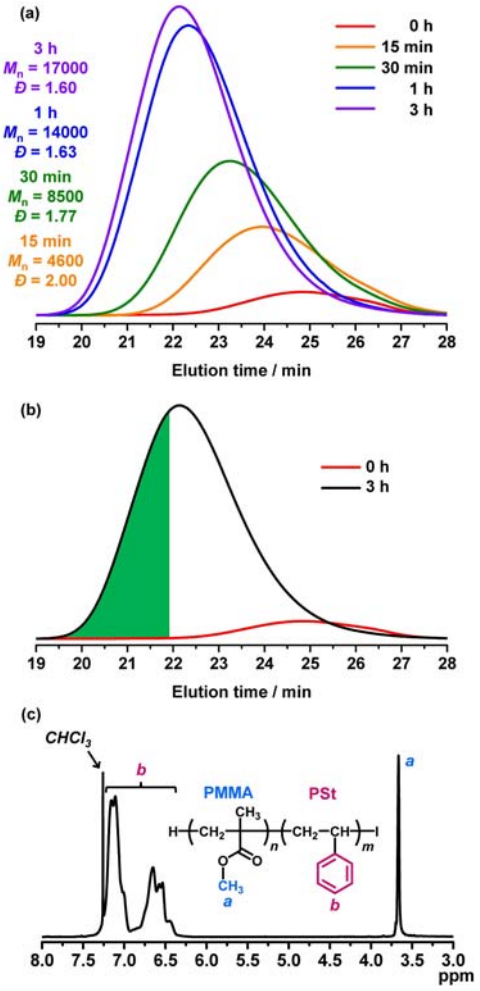

Fig. 5 (a) GPC chromatograms for the St/PMMA–Y/CP–I/PBZ system (120 °C). The reaction condition is given in Table 2 (entry 1). (b) GPC chromatograms at t = 0 and 3 h. (c) ^{1}H NMR spectrum of the fractionated polymer (green area in (b)).

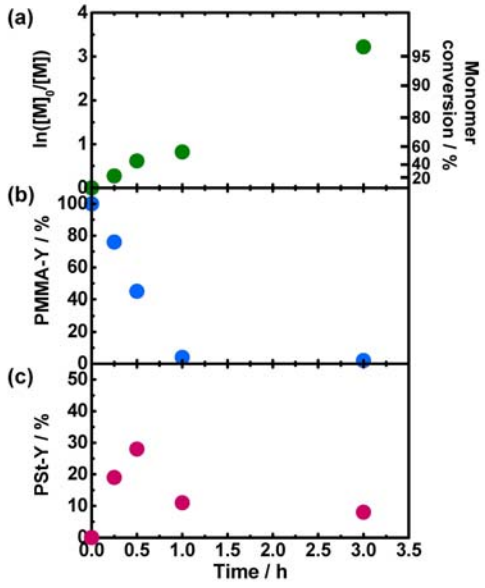

Fig. 6 Plots of (a) $\ln([M]_0/[M])$, (b) fraction of PMMA–Y, and (c) fraction of PSt–Y vs time t for the St/PMMA–Y/CP–I/PBZ system (120 °C) (Table 2 (entry 1)).

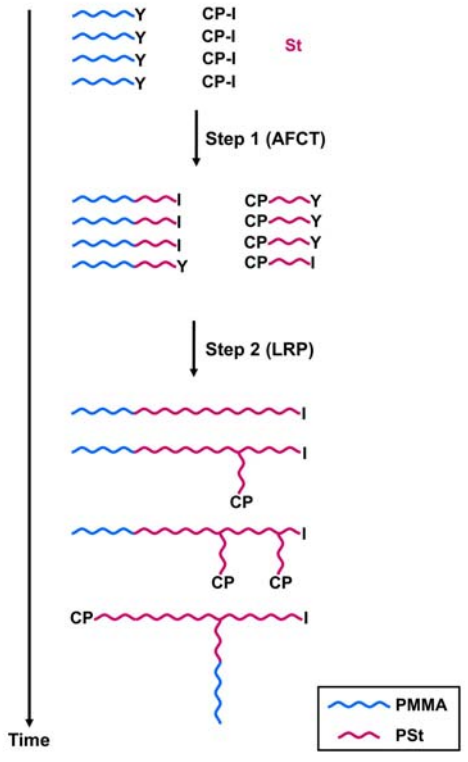

Scheme 3 Schematic illustration for the generation of block copolymer from PMMA–Y.

Viscosity and composition analysis

In the St system, PMMA–Y works as a macroinitiator and tends to generate linear PMMA–PSt block copolymers at 120 °C (F_{fr} ~ 100%), although some block copolymers can have branches in the PSt segment (Scheme 3). In contrast, at 40 °C (F_{fr} = 13%), PMMA–Y works as a macromonomer and tends to generate more branched polymers with the PS main chain and PMMA branches. Therefore, interestingly, we tend to obtain block and branched copolymers by just changing temperature.

To confirm the structural difference, we measured intrinsic viscosity [η] for a polymer synthesized at 120 °C (M_n = 17000, $Đ$ = 1.60, conv = 96%) (Table 2 (entry 1) at 3 h) and a polymer synthesized at 40 °C (M_n = 15000, $Đ$ = 1.51, conv = 90%) (Table 2 (entry 2) at 16 h). Because the M_n and $Đ$ values are similar, a difference in [η] will result from the linear and branched structures. Fig. 7 shows the Mark-Houwink plot. The [η] value for the polymer at 120 °C was larger than that for the polymer at 40 °C by 18–33% in the studied range of molecular weight (12000–63000), supporting that the polymer synthesized at 120 °C tends to be more linear than that synthesized at 40 °C.

The St/MMA composition of the polymer obtained at 120 °C was analyzed with gradient polymer elution chromatography (GPEC) (Fig. 8). In GPEC, polymers are separated based on their polarity with a gradient eluent of acetonitrile/tetrahydrofuran (THF) (from 100/0 to 0/100). The dashed and dotted lines show a pure PMMA (PMMA–Y) with a peak at 4.2 min and a pure PSt (GPC standard PSt (M_n = 19000 and $Đ$ = 1.01)) with a peak at 7.9 min, respectively. After the 3 h polymerization, the peak for PMMA–Y at 4.2 min almost disappeared, which is consistent with the NMR result (Fig. 6b). Instead, we observed a new peak at 6.5–7.7 min, i.e., between 4.2 min (pure PMMA) and 7.9 min (pure PSt), corresponding to PMMA–PSt block copolymers. This result confirms the generation of the copolymer. We also observed a PSt homopolymer (remaining PSt–Y (Fig. 6c)) at 7.8 min. The integral (not the peak height) at 6.5–7.7 min (for block copolymer) is much larger than that at 7.8 min (for PSt homopolymer), agreeing with the generation of block copolymers as main components.

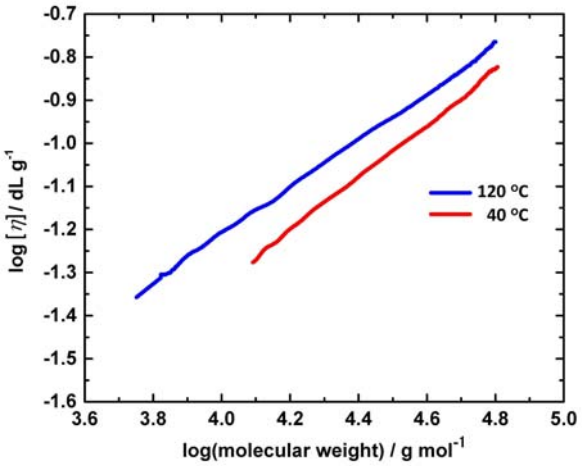

Fig. 7 Mark-Houwink plot of the PMMA–PSt polymers synthesized at 40 °C and 120 °C.

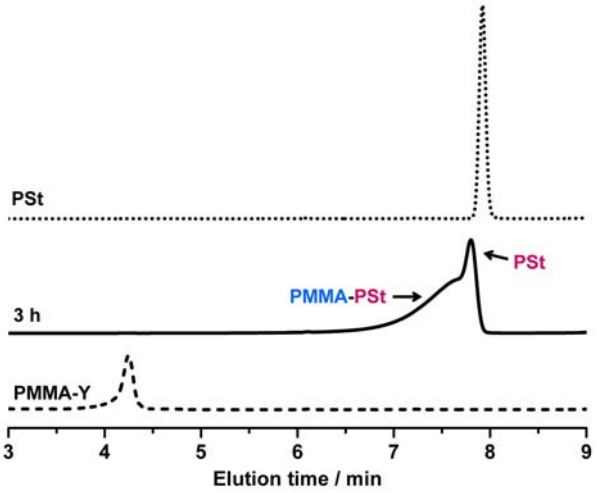

Fig. 8 GPEC chromatograms for a pure PSt, the polymer obtained after 3 h at 120 °C (Table 2 (entry 1)), and a pure PMMA (PMMA–Y).

Determination of F_{fr} for PAN$^{\bullet}$ and block polymerization of AN from PMMA–Y.

We studied a polymerization of AN (200 equiv) with PMMA–Y (M_n = 3900 and $Đ$ = 1.67) (1 equiv), 2,2′-azobis(isobutyronitrile) (AIBN) (0.1 equiv), CP–I (1 equiv), and BNI (4 equiv) in ethylene carbonate (EC) (solvent, 50 wt%) at 75 °C (Table 2 (entry 3)). The system is RCMP using CP–I as an alkyl iodide dormant species and BNI as a catalyst. The temperature selected (75 °C) is suitable for the polymerization of AN *via* RCMP.[11] AIBN was added to increase the polymerization rate. EC was a solvent to dissolve the PAN segment. The obtained polymers were purified by reprecipitation.

Fig. 9 shows the ^{1}H NMR spectra (DMSO-d_6) of the polymers obtained at time zero (Fig. 9a) and 1 h (Fig. 9b, monomer conversion = 46%). The CH_2=C protons of PMMA–Y appeared at 5.52–5.60 and 6.08–6.17 ppm (Fig. 9a). At 1 h, two new peaks appeared at 5.90–5.95 and 6.28–6.31 ppm and corresponded to the CH_2=C protons of PAN–Y (Fig. 9b). The F_{fr} value obtained from the peak areas was 97% (Table 1 (entry 2) and Fig. S2 in the ESI), meaning that the PAN–(Y$^{\bullet}$)–PMMA intermediate undergoes fragmentation (AFCT) predominantly over propagation.

Because of the predominant AFCT, we were able to obtain PMMA–PAN block copolymers in this system. The GPC curves smoothly shifted from the low molecular weight side to the high molecular weight side (Fig. S3 in the ESI). The first order plot of the monomer concentration was linear (Fig. 10a). After 7 h, the monomer conversion reached 86%, M_n was 15000, $Đ$ was 1.82 (Table 2 (entry 3)), and 88% of PMMA–Y was consumed (Fig. 10b), suggesting that a large amount of

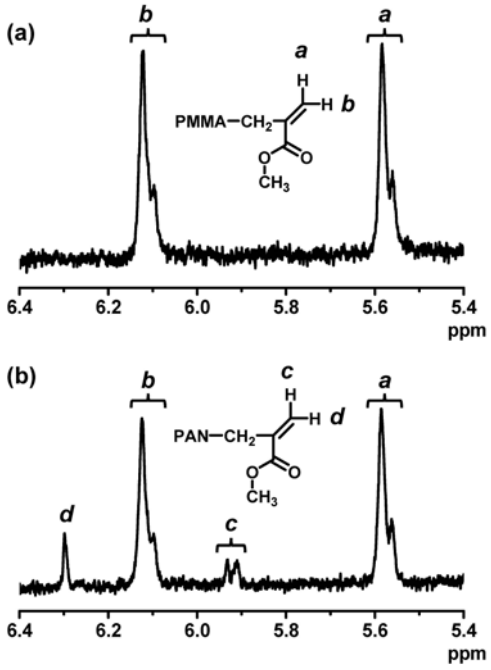

Fig. 9 ^{1}H NMR spectra (DMSO-d_6) in the range of 5.4–6.4 ppm at t = (a) 0 and (b) 1 h for the AN/PMMA–Y/CP–I/AIBN/BNI system (75 °C). The reaction condition is given in Table 2 (entry 3).

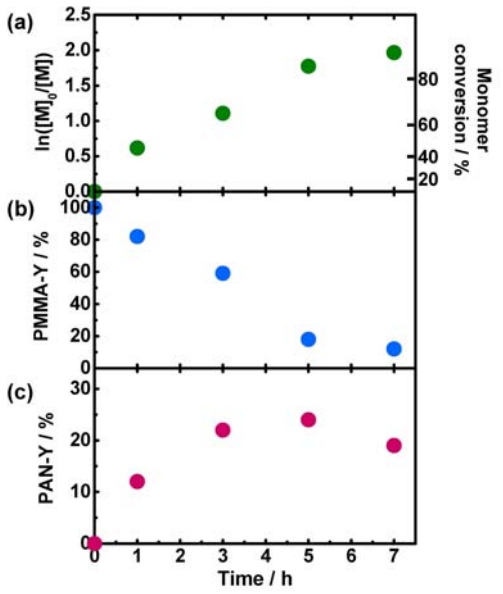

Fig. 10 Plots of (a) ln([M]$_0$/[M]), (b) fraction of PMMA–Y, and (c) fraction of PAN–Y vs time t for the AN/PMMA–Y/CP–I/AIBN/BNI system (75 °C). The reaction condition is given in Table 2 (entry 3).

PMMA–Y became PMMA–PAN block copolymers. PAN–Y was accumulated and turned to decay after 5 h (Fig. 10c) similarly to the St polymerization.

Block polymerizations of functional acrylates from PMMA–Y.

We previously reported an RCMP of BA using PMMA–Y to synthesize PMMA–PBA block copolymers. The F_{fr} value is >90% for acrylates (as mentioned above), rationalizing the formation of PMMA–PBA block copolymers. In the present work, we expanded the monomer scope to functional acrylates, i.e., hydrophobic methoxyethyl acrylate (MEA) and amphiphilic poly(ethylene glycol) methyl ether acrylate (PEGA) (molecular weight = 480 g mol^{-1}), both of which are biocompatible acrylate monomers (Fig. 1). We carried out bulk RCMPs of these monomers (100 or 200 equiv) with PMMA–Y (1 equiv), CP–I (1 equiv), and BNI (8 equiv) at 110°C (Table 2 (entries 4 and 5)). The relatively high temperature of 110 °C was required for RCMP of acrylates because the secondary carbon-iodine bonds are relatively strong and cleavable at high temperatures with BNI catalyst.[11] The GPC curve shifted over time for both MEA (Fig. 11) and PEGA (Fig. S4 in the ESI). After 24 h, we obtained polymers with M_n = 15000 and $Đ$ = 1.96 for MEA (monomer conversion = 72%) and M_n = 13000 and $Đ$ = 1.53 for PEGA (monomer conversion = 41%). 86% of PMMA–Y was consumed after 24 h in both polymerizations (Fig. 12b and Fig. S5b in the ESI). PMEA–Y (Fig. S6 in the ESI) and PPEGA–Y (Fig. S7 in the ESI) accumulated to nearly the same extent that PMMA–Y was consumed in the first 2–4 h (Fig. 12c and Fig. S5c in the ESI). The F_{fr} value was determined to be ~100% for PMEA and 83% for PPEGA (Table 1 (entries 3 and 4)), showing high efficiencies of AFCT to obtain block copolymers. These results demonstrate the use of PMMA–Y and functional acrylates to have access to block copolymers.

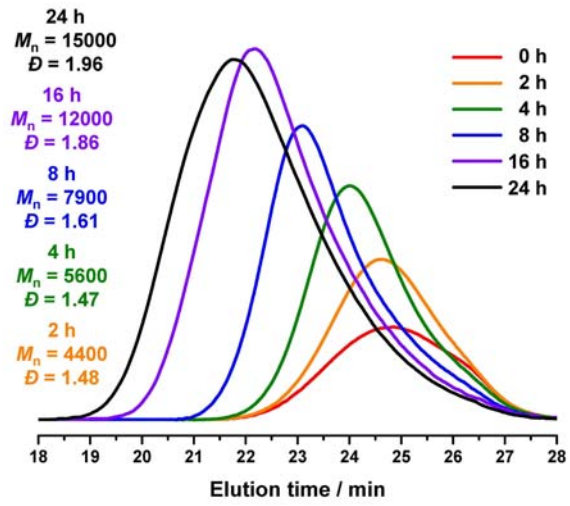

Fig. 11 GPC chromatograms for the MEA/PMMA–Y/CP–I/BNI system (110 °C). The reaction condition is given in Table 2 (entry 4).

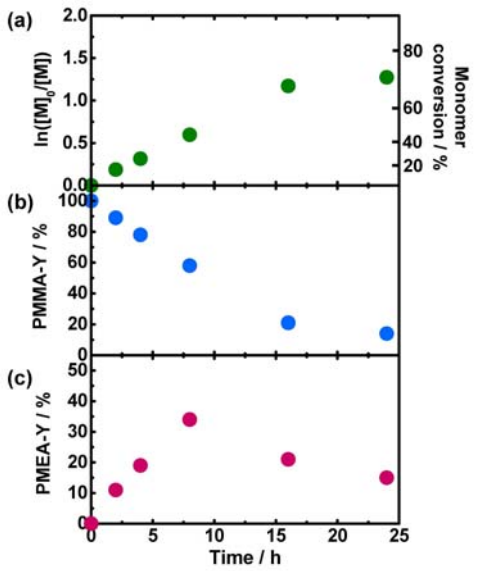

Fig. 12 Plots of (a) ln([M]$_0$/[M]), (b) fraction of PMMA–Y, and (c) fraction of PMEA–Y vs time *t* for the MEA/PMMA–Y/CP–I/BNI system (110 °C) (Table 2 (entry 4)).

Use of I_2 and an azo compound.

Instead of using an isolated alkyl iodide (CP–I), we may use molecular iodine (I_2) and an azo compound (AIBN or 2,2'-azobis(2,4-dimethylvaleronitrile) (V65)) as starting compounds to generate an alkyl iodide *in situ* in the polymerization. The azo compound (R-N=N-R) generates an alkyl radical ($R^{\bullet}$), which then reacts with I_2 to produce an alkyl iodide (R–I). This I_2/azo method was initially developed in ITP[6,17,34,35] and subsequently used in RCMP.[11,36] This method is attractive for practical use, because I_2 and AIBN are inexpensive. In the present work, we used the I_2/azo method for the polymerizations of St, AN, MEA, and PEGA using PMMA–Y. We heated a mixture of monomer (100 or 200 equiv), PMMA–Y (1 equiv), I_2 (0.5 equiv), an azo compound (0.72–1.1 equiv), and BNI at 75–120 °C (Table 3). Because the efficiency of an azo compound to produce free $R^{\bullet}$ is not unity, an excess of the azo compound (0.72–1.1 equiv) to I_2 (0.5 equiv) was added to ensure that I_2 was quantitatively converted to R–I. BNI was absent for St (ITP) and present for AN, MEA, and PEGA (RCMP). The azo compound completely decomposed within 1 h at the studied temperatures, during which time $R^{\bullet}$ would predominantly react with I_2 (rather than the monomer) and R–I accumulated. The monomer conversion reached 54–93% in the studied polymerization time (3–24 h), and a large fraction (78–99%) of PMMA–Y was consumed to generate block copolymers (Table 3). The polymerization was controlled similarly to that in the CP–I system (Table 2) in all cases, demonstrating the effectiveness of the I_2/azo approach. Again, this method is robust because of no requirement of the isolation of R–I.

Use of PMMA–Y with higher molecular weight

We also used a PMMA–Y with a higher molecular weight, i.e., M_n = 12000 and Đ = 1.78, in the BA polymerization. We carried out RCMP of BA (300 equiv) using PMMA–Y (1 equiv), CP–I (1 equiv) and BNI (8 equiv) at 110 °C (Table 4 and Fig. 13). The polymerization virtually completed after 72 h (monomer conversion = 97%), yielding a polymer with M_n = 38000 and Đ = 3.43 (Table 4 and Fig. S8 in the ESI). Interestingly, despite the higher molecular weight of PMMA–Y, a large amount (85%) of PMMA–Y was consumed to generate a PMMA–PBA block copolymer after 72 h (Fig. 13b).

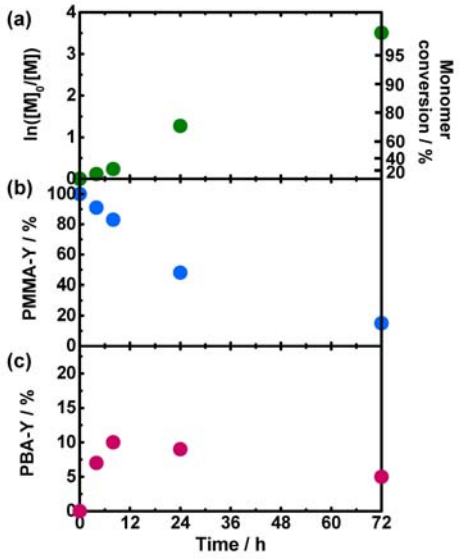

Fig. 13 Plots of (a) ln([M]$_0$/[M]), (b) fraction of PMMA–Y, and (c) fraction of PBA–Y vs time *t* for the BA/PMMA–Y/CP–I/BNI system (110 °C). The reaction condition is given in Table 4.

Table 3. Polymerizations of St, AN, MEA and PEGA with PMMA–Y (M_n = 3900 and $Đ$ = 1.67) using azo compound and iodine.

Entry	monomer	azo	[Monomer]$_0$/[PMMA–Y]$_0$/[I_2]$_0$/[azo]$_0$/[BNI]$_0$ (mM)	T (°C)	t (h)	Conv (%)	M_n[a] ($M_{n,theo}$[b])	$Đ$[a]	PMMA–Y remaining (%)
1	St	AIBN	8000/40/20/28.8/0[c]	120	3	93	15000 (23000)	1.73	1
2	AN	V65/AIBN	8000/40/20/(28.8/4)/160[d]	75	7	81	13000 (12000)	2.30	22
3	MEA	AIBN	8000/40/20/30/320	110	24	93	15000 (28000)	1.78	15
4	PEGA	AIBN	8000/80/40/88/640[d]	110	24	54	15000 (30000)	1.67	22

[a]PMMA-calibrated GPC values. The eluent was tetrahydrofuran (THF) for entries 1 and 3 and dimethylformamide (DMF) for entries 2 and 4. [b]Theoretical M_n calculated with [monomer]$_0$, [PMMA–Y]$_0$, and monomer conversion. [c]With PBZ (60 mM). [d]Diluted in 50 wt% ethylene carbonate (EC) to dissolve the PAN segment for entry 2 and 10 wt% diglyme to dissolve AIBN for entry 4.

Table 4. Polymerization of BA with PMMA–Y (M_n = 12000 and $Đ$ = 1.78) (110 °C).

[BA]$_0$/[PMMA–Y]$_0$/[CP–I]$_0$/[BNI]$_0$ (mM)	t (h)	Conv (%)	M_n[a] ($M_{n,theo}$[b])	$Đ$[a]
8000/27/27/213	4	11	10000 (16000)	1.94
	8	21	12000 (20000)	1.75
	24	72	27000 (40000)	2.63
	72	97	38000 (49000)	3.43

[a]PMMA-calibrated THF-GPC values. [b]Theoretical M_n calculated with [monomer]$_0$, [PMMA–Y]$_0$, and monomer conversion.

Conclusions

The F_{fr} of PMMA–Y in the St polymerization strongly depended on temperature and ranged from 13% at 40 °C to approximately 100% at 120 °C. PMMA–Y mainly worked as a macromonomer to generate branched polymers at 40 °C and predominantly worked as a macroinitiator to generate PMMA–PS block copolymers at 120 °C. Such a selective generation would be interesting. Based on this finding, PMMA–PS block copolymers were synthesized at 120 °C *via* ITP. The F_{fr} values were also high (80–99%) for AN, MEA, and PEGA. The block copolymers were obtained in RCMP (with BNI catalyst) for AN, MEA, and PEGA. For all studied monomers, not only the isolated CP–I but also the alkyl iodide *in situ* generated from I_2 and azo compound was effectively used as the initiating dormant species. The *in situ* method is less expensive and robust and hence can be a practically attractive alternative. The RCMP of BA was extended onto a higher molecular weight PMMA–Y. Despite a longer PMMA chain, a large amount (85%) of PMMA–Y was consumed to produce PMMA–PBA block copolymers.

Conflicts of interest

There are no conflicts to declare.

Acknowledgements

This work was supported by National Research Foundation (NRF) Investigatorship in Singapore (NRF-NRFI05-2019-0001) and Academic Research Fund (AcRF) Tier 2 from Ministry of Education in Singapore (MOE2017-T2-1-018).

References

1 K. Matyjaszewski, *Adv. Mater.*, 2018, **30**, 1706441.
2 J. Nicolas, Y. Guillaneuf, C. Lefay, D. Bertin, D. Gigmes and B. Charleux, *Prog. Polym. Sci.*, 2013, **38**, 63–235.
3 K. Matyjaszewski and N. V. Tsarevsky, *J. Am. Chem. Soc.*, 2014, **136**, 6513–6533.
4 M. Ouchi and M. Sawamoto, *Macromolecules*, 2017, **50**, 2603–2614.
5 D. J. Keddie, G. Moad, E. Rizzardo and S. H. Thang, *Macromolecules*, 2012, **45**, 5321–5342.
6 G. David, C. Boyer, J. Tonnar, B. Ameduri, P. Lacroix-Desmazes and B. Boutevin, *Chem. Rev.*, 2006, **106**, 3936–3962.
7 P. B. Zetterlund, S. C. Thickett, S. Perrier, E. Bourgeat-Lami and M. Lansalot, *Chem. Rev.*, 2015, **115**, 9745–9800.
8 S. Yamago, *Chem. Rev.*, 2009, **109**, 5051–5068.
9 A. Goto and T. Fukuda, *Prog. Polym. Sci.*, 2004, **29**, 329–385.
10 A. Goto, H. Zushi, N. Hirai, T. Wakada, Y. Tsujii and T. Fukuda, *J. Am. Chem. Soc.*, 2007, **129**, 13347–13354.
11 A. Goto, A. Ohtsuki, H. Ohfuji, M. Tanishima and H. Kaji, *J. Am. Chem. Soc.*, 2013, **135**, 11131–11139.
12 A. Ohtsuki, L. Lei, M. Tanishima, A. Goto and H. Kaji, *J. Am. Chem. Soc.*, 2015, **137**, 5610–5617.
13 C.-G. Wang and A. Goto, *J. Am. Chem. Soc.*, 2017, **139**, 10551–10560.
14 C.-G. Wang, F. Hanindita and A. Goto, *ACS Macro Lett.*, 2018, **7**, 263–268.
15 X. Liu, C.-G. Wang and A. Goto, *Angew. Chem. Int. Ed.* 2019, **58**, 5598–5603.
16 H. Xu, C.-G. Wang, Y. Lu and A. Goto, *Macromolecules*, 2019, **52**, 2156−2163.
17 C. Boyer, P. Lacroix-Desmazes, J.-J. Robin and B. Boutevin, *Macromolecules*, 2006, **39**, 4044–4053.
18 J. J. Chang, L. Xiao, C.-G. Wang, H. Niino, S. Chatani and A. Goto, *Polym. Chem.*, 2018, **9**, 4848–4855.
19 A. A. Gridnev, *Polym. J.*, 1992, **24**, 613–623.
20 K. J. Abbey, D. L. Trumbo, G. M. Carlson, M. J. Masola and R. A. Zander, *J. Polym. Sci., Part A: Polym. Chem.*, 1993, **31**, 3417–3424.
21 D. M. Haddleton, D. R. Maloney and K. G. Suddaby, *Macromolecules*, 1996, **29**, 481–483.
22 K. G. Suddaby, D. M. Haddleton, J. J. Hastings, S. N. Richards and J. P. O'Donnell, *Macromolecules*, 1996, **29**, 8083–8091.
23 J. P. A. Heuts and N. M. B. Smeets, *Polym. Chem.*, 2011, **2**, 2407–2423.
24 J. Krstina, G. Moad, E. Rizzardo, C. L. Winzor, C. T. Berge and M. Fryd, *Macromolecules*, 1995, **28**, 5381–5385.
25 C. L. Moad, G. Moad, E. Rizzardo and S. H. Thang, *Macromolecules*, 1996, **29**, 7717–7726.

26 B. Yamada, F. Oku and T. Harada, *J. Polym. Sci., Part A: Polym. Chem.*, 2003, **41**, 645–654.
27 B. Yamada, P. B. Zetterlund and E. Sato, *Prog. Polym. Sci.*, 2006, **31**, 835–877.
28 G. Moad, E. Rizzardo and S. H. Thang, *Polymer*, 2008, **49**, 1079–1131.
29 D. Zhou, R. P. Kuchel and P. B. Zetterlund, *Polym. Chem.*, 2017, **8**, 4177–4181.
30 N. G. Engelis, A. Anastasaki, G. Nurumbetov, N. P. Truong, V. Nikolaou, A. Shegiwal, M. R. Whittaker, T. P. Davis and D. M. Haddleton, *Nat. Chem.*, 2016, **9**, 171–178.
31 I. Schreur-Piet and J. P. A. Heuts, *Polym. Chem.*, 2017, **8**, 6654–6664.
32 N. G. Engelis, A. Anastasaki, R. Whitfield, G. R. Jones, E. Liarou, V. Nikolaou, G. Nurumbetov and D. M. Haddleton, *Macromolecules*, 2018, **51**, 336–342.
33 B. Yamada, S. Kobatake and S. Aoki, *Macromol. Chem. Phys*., 1994, **195**, 581–590.
34 P. Lacroix-Desmazes, R. Severac and B. Boutevin, *Macromolecules*, 2005, **38**, 6299–6309.
35 For another synthetic method to generate an alkyl iodide in situ in a polymerization, J. Tonnar and P. Lacroix-Desmazes, *Angew. Chem. Int. Ed.*, 2008, **47**, 1294–1297.
36 For another synthetic method to generate an alkyl iodide in situ in a polymerization, L. Xiao, K. Sakakibara, Y. Tsujii and A. Goto, *Macromolecules*, 2017, **50**, 1882–1891.

Graphical Abstract

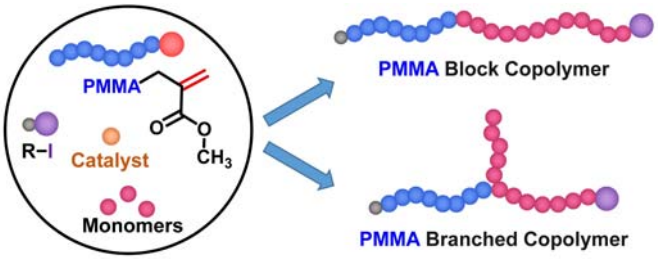

Kinetic studies aided the controlled synthesis of PMMA block copolymers and PMMA branched copolymers from a PMMA containing an unsaturated chain end.